

---

This is an electronic reprint of the original article.  
This reprint may differ from the original in pagination and typographic detail.

Ahmad, Bilal; Kyyra, Jorma; Martinez, Wilmar

## Efficiency optimisation of an interleaved high step-up converter

*Published in:*  
The Journal of Engineering

*DOI:*  
[10.1049/joe.2018.8040](https://doi.org/10.1049/joe.2018.8040)

Published: 01/06/2019

*Document Version*  
Publisher's PDF, also known as Version of record

*Published under the following license:*  
CC BY

*Please cite the original version:*  
Ahmad, B., Kyyra, J., & Martinez, W. (2019). Efficiency optimisation of an interleaved high step-up converter. *The Journal of Engineering*, (17), 4167-4172. <https://doi.org/10.1049/joe.2018.8040>

---

This material is protected by copyright and other intellectual property rights, and duplication or sale of all or part of any of the repository collections is not permitted, except that material may be duplicated by you for your research use or educational purposes in electronic or print form. You must obtain permission for any other use. Electronic or print copies may not be offered, whether for sale or otherwise to anyone who is not an authorised user.

# Efficiency optimisation of an interleaved high step-up converter

eISSN 2051-3305  
Received on 21st June 2018  
Accepted on 27th July 2018  
E-First on 15th April 2019  
doi: 10.1049/joe.2018.8040  
www.ietdl.org

Bilal Ahmad<sup>1</sup>, Jorma Kyra<sup>1</sup>, Wilmar Martinez<sup>2,3</sup> ✉

<sup>1</sup>Department of Electrical and Automation Engineering, Aalto University, Espoo, Finland

<sup>2</sup>Department of Electrical Engineering (ESAT), Diepenbeek Campus, KU Leuven, Belgium

<sup>3</sup>EnergyVille, Genk, Belgium

✉ E-mail: wilmar.martinez@kuleuven.be

**Abstract:** This study presents the performance comparison of two scenarios to obtain high voltage gain. A high step-up converter (HSU) and a cascaded boost converter are chosen for this study. For analytical analysis, a loss model for both converters is developed on MATLAB. Gallium nitride-based prototypes of HSU and cascade boost converter provided the validation of the analytical analysis. Based on the theoretical evaluation and practical tests, efficiencies of both converters are expressed in terms of their voltage gain to find the optimal point of operation. Results showed that the cascaded boost converter is more efficient than the HSU converter at higher voltage gain values. However, the HSU converter has a higher energy density and lower switch voltage stress than those of the cascaded boost converter.

## 1 Introduction

Over the years, with the increasing global power demand and rising global temperature, photo-voltaic (PV) applications have gained more and more interest [1]. Conventionally huge solar parks are connected to grid through various parallel central solar inverters [2]. Central inverters offer an efficient solution with high power density [3]. However, various drawbacks of this family of inverters include losses due to partial shading of solar module, poor expansion flexibility and electric hazards due to high DC voltage [4]. To avoid these problems, string inverters are employed. Instead of connecting a large number of solar panels to a central inverter, a string of modules is connected to their specific inverter [5]. Though string inverters resolve the aforementioned problems, high DC voltage of a string of solar modules and flexibility for expansion still pose challenges [2].

These problems are further reduced by the application of a modular solar inverter. Each solar module is equipped with its individual MPPT and a DC/AC inverter [6, 7]. In these solar inverters, the available DC voltage from a solar panel is very low [8]. High gain DC-DC converters are essential to boost the PV voltage to a level that is required to generate AC grid voltage [9]. Conventional boost converters cannot be used in such applications because of their inability to provide such high gain [10]. Higher gain means that boost converters will have to operate at a higher duty cycle around 0.9, which makes it inefficient and impossible to get in some extreme cases. However, input current in an interleaved boost converter is divided into two or more phases that reduce the losses of the converter [11]. However, if a voltage gain of  $>5$  is required, high step-up topologies are needed [12, 13]. Martinez *et al.* [14] presented a HSU converter with a higher gain than that of the conventional interleaved boost converter. This converter utilises the concept of interleaved phase and magnetic coupling to achieve very high gain [15, 16]. This attribute makes it an excellent choice for a modular PV inverter wherein high voltage gain is required. However, this HSU converter introduces an additional magnetic component and two diodes. It makes the operation more complicated and also increases the losses. Another simpler way of obtaining high voltage gain is using a two-stage interleaved cascaded boost converter. However, this approach has more switching devices and lesser energy density than those of the HSU converter.

In order to find an optimised solution, the performance of the HSU converter has been compared with that of the cascaded

interleaved boost converter. For analytical analysis, a comprehensive loss model has been developed for the switching and magnetic components for both converters. Practical prototypes rated at 250 W have been developed to validate the theoretical reasoning. Performances of the HSU and cascaded boost converters are evaluated for fixed output voltage at different switching frequencies and input voltage levels.

This paper is organised as follows: Section 2 explains the different modes of operation of the proposed high step-up converter. Section 3 gives the analytical analysis of the performance comparison of HSU and cascaded interleaved boost converters. Section 4 includes the results from experimental tests. Conclusion is drawn in Section 5.

## 2 Modified high step-up converter

Fig. 1 presents the high step-up converter proposed in [14]. This HSU converter consists of an additional winding  $L_C$  as compared to the two-phase interleaved boost converter. This converter also consists of two additional diodes. Like the interleaved boost converter, windings  $L_1$  and  $L_2$  are connected to the input DC voltage source. Switches  $S_1$  and  $S_2$  are connected to windings  $L_1$  and  $L_2$ , respectively. Both switches are switched ON at the same switching frequency and duty cycle, while they are  $180^\circ$  out of phase. Central winding  $L_C$  is connected to  $L_1$  and  $L_2$  through diodes  $D_1$  and  $D_2$ . As all three windings are coupled, they can be wound on a single core. Fig. 2 shows the structure of all three windings wound on a single core.

Different modes of conduction for duty cycles  $D < 0.5$  and  $D > 0.5$  are shown in Figs. 3a and Fig. 3b, respectively. To develop a loss model for the converter, it is important to find the relation for the average value of the current during different conduction states.

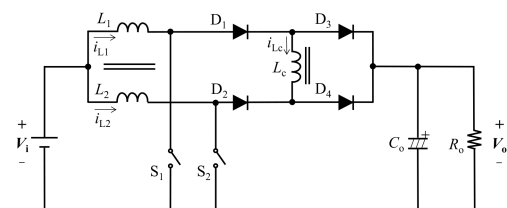
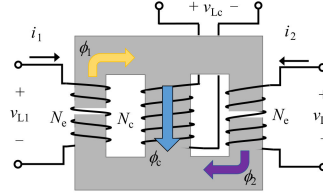
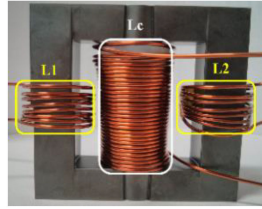
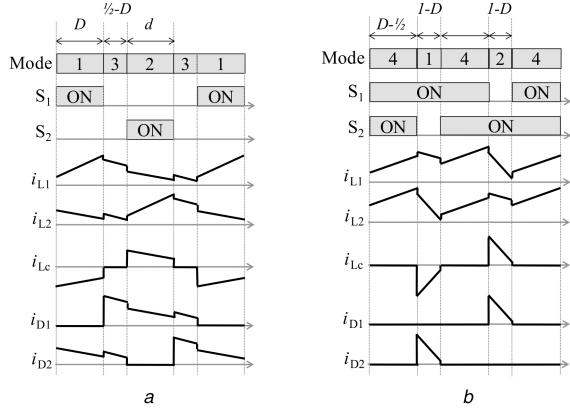


Fig. 1 Modified HSU converter



**Fig. 2** Coupled inductors on a single core



**Fig. 3** Modes of operation

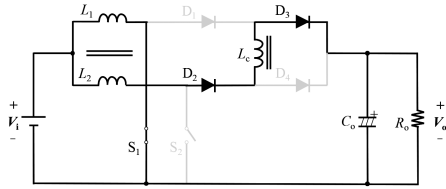


**Fig. 4** Mode 1 – conduction diagram

### 2.1 Mode 1

During this mode, switch  $S_1$  is switched ON, while  $S_2$  is switched OFF. Fig. 4 shows the conduction diagram for this mode.

As winding  $L_1$  is directly connected to the input voltage

$$v_{L1} = v_i \quad (1)$$

$$v_{L2} = \frac{v_i(1+N) - v_o}{(1+N)} \quad (2)$$

where  $N$  is the ratio of turns of central winding  $L_C$  to winding  $L_1$  or  $L_2$ , and  $v_o$  is the output voltage. Keeping in mind that all conductors are coupled, after doing basic calculations, the rate of change of current in inductors is given as follows:

$$\frac{di_{L1,MOD_1}}{dt} = \frac{v_i(1+N)(M-L-2M_c) - v_o(M-M_c)}{(1+N)(M+L)(M-M_c-L)} \quad (3)$$

$$\frac{di_{L2,MOD_1}}{dt} = \frac{v_i(1+N)(M-L) + v_oL}{(1+N)(M+L)(M-M_c-L)} \quad (4)$$

where  $M$  is mutual inductance between  $L_1$  and  $L_2$ , while  $M_c$  is mutual inductance between  $L_C$  and the external windings  $L_1$  and  $L_2$ . The inductance of both  $L_1$  and  $L_2$  is equal; hence,  $L_1 = L_2 = L$ .

The average value of the current through  $L_1$  and  $L_2$  can be calculated by integrating (3) and (4) over the time period of mode 1, i.e.  $D/f_s$ , where  $D$  is the duty cycle and  $f_s$  is the switching frequency.  $I_{L1(0)}$  and  $I_{L2(0)}$  are the values of current in  $L_1$  and  $L_2$  at the beginning of the mode:

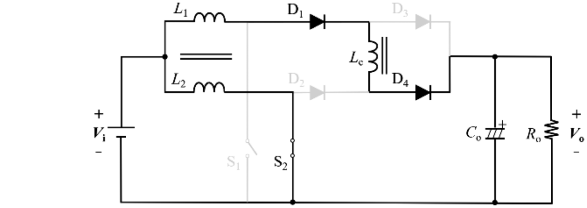


**Fig. 5** Mode 2 – conduction diagram

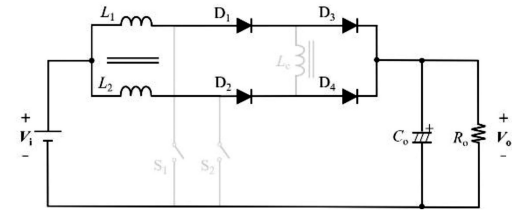


**Fig. 6** Mode 3 – conduction diagram

$$I_{L1,MOD_1} = \frac{(v_i(1+N)(M-L-2M_c) - v_o(M-M_c))D}{((1+N)(M+L)(M-M_c-L))f_s} + I_{L1(0)} \quad (5)$$

$$I_{L2,MOD_1} = \frac{(v_i(1+N)(M-L) + v_oL)D}{((1+N)(M+L)(M-M_c-L))f_s} + I_{L2(0)} \quad (6)$$

### 2.2 Mode 2

During Mode 2,  $S_1$  is switched OFF, while  $S_2$  is switched ON. The conduction diagram for this mode is shown in Fig. 5.

During this mode, current equations are as follows:

$$\frac{di_{L1,MOD_2}}{dt} = \frac{di_{L2,MOD_1}}{dt} \quad (7)$$

$$\frac{di_{L2,MOD_2}}{dt} = \frac{di_{L2,MOD_1}}{dt} \quad (8)$$

As duration of modes 1 and 2 is equal, so

$$I_{L1,MOD_2} = I_{L2,MOD_1} \quad (9)$$

$$I_{L1,MOD_2} = I_{L2,MOD_1} \quad (10)$$

### 2.3 Mode 3

During this mode of operation, both switches  $S_1$  and  $S_2$  are switched OFF. Fig. 6 gives the equivalent circuit diagram during this mode of operation. Current through the windings  $L_1$  and  $L_2$  can be given by (11) and (12):

$$I_{L1,MOD_3} = \frac{v_i - v_o}{L+M} \frac{1-2D}{f_s} + I_{L1(0)} \quad (11)$$

$$I_{L2,MOD_3} = I_{L1,MOD_3} \quad (12)$$

In Fig. 3, the duration of mode 3 in each cycle is  $1-2D$ , where  $D$  is the duty ratio.

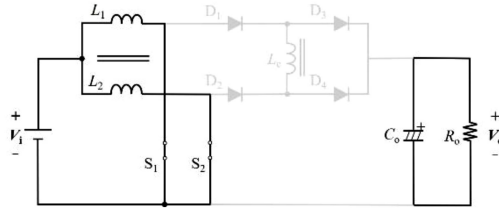


Fig. 7 Mode 4 – conduction diagram

Table 1 Simulation parameters

output power	$P_o$	1 kW
output voltage	$V_o$	200 V
switching frequency	$f_s$	100 kHz
inductance external legs	$L_1 = L_2$	302 $\mu$ H
inductance middle leg	$L_c$	2.22 mH
Steinmetz constants (PC40)	$K$	$4.5 \times 10^{-14}$
	$\alpha$	2.5
	$\beta$	1.55
turns ratio	$N_c/N_1$	2
winding resistance	$R_L$	1.10 $\Omega$
load resistance	$R_o$	160 $\Omega$

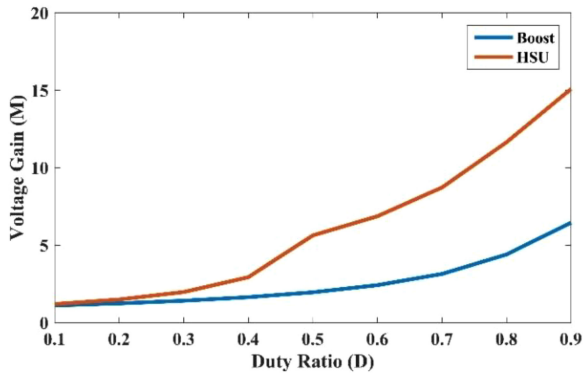


Fig. 8 Duty ratio vs. voltage gain

#### 2.4 Mode 4

When the duty ratio of  $>0.5$  will be required, instead of mode 3, converter will operate in mode 4. During mode 4, both switches  $S_1$  and  $S_2$  are switched ON. Fig. 7 shows the conduction diagram of the converter during this mode.

Duration of mode 4 is  $2D - 1$ ; hence, current equations for this mode will be as follows:

$$I_{L1,MOD_4} = \frac{v_i}{L + M} \frac{2D - 1}{f_s} + I_{L1(0)} \quad (13)$$

$$I_{L1,MOD_3} = I_{L2,MOD_3} \quad (14)$$

### 3 Analytical analysis

Solar modules are rated at low DC voltage with maximum power point voltage of around 24 VDC. With the conventional interleaved boost converter, gain is limited. With the analysis made in [17], it is possible to express the gain of the conventional interleaved boost converter and the HSU converter in terms of duty cycle. Equation (15) gives the gain of the conventional boost converter, while (16) and (17) give gain of the HSU converter for  $D < 0.5$  and  $D > 0.5$ , respectively:

$$M_{BOOST} = \frac{1}{(1 - D) + (1 + (R_L / (R_o(1 - D)^2)))} \quad (15)$$

(see (16))

$$M_{HSU_{D < 0.5}} = \frac{1 + N}{1 - D + (R_L / R_o)((1 + N - ND)(1 + N) / 2(1 - D))} \quad (17)$$

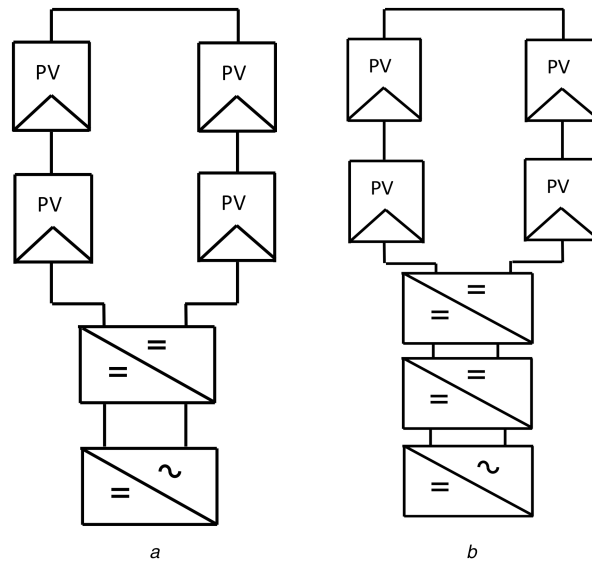
where  $R_L$  and  $R_o$  are the resistance of inductor and load resistance, respectively. To find an optimised point of operation, a loss model based on parameters mentioned in Table 1 has been developed in MATLAB.

Fig. 8 shows the comparison of the HSU converter with the conventional interleaved converter in terms of voltage gain.

It is evident that applications (solar cells, fuel cells) where a low-voltage high-current source must be converted into a high-voltage low-current source, the HSU converter has its advantages. With the conventional boost converter, the maximum gain that can be achieved at the duty ratio of 0.9 is 6.5, while with the HSU converter, a gain of 15.1 can be achieved with parameters defined in Table 1. Fig. 9 shows the two different configurations of PV applications. In Fig. 9a, a higher gain is achieved by the application of the HSU converter; however in Fig. 9b, two conventional interleaved boost converters are used to achieve the higher voltage gain.

Solar panels are usually rated at open circuit voltage of 36 V and even lower voltage level for maximum power point [4]. With solar panels rated at 20  $V_{MPP}$ , the configuration shown in Fig. 9 with two panels in series would require a gain of 10 to step-up the voltage level to 400 VDC. With the HSU converter, a gain of 10 can be achieved around a duty ratio of 0.8. In comparison, two conventional interleaved boost converters would be required. Each boost converter provides the gain of 5, and they are cascaded at the common DC bus of the inverter. Fig. 10 shows the efficiency comparison of the cascaded boost converter and HSU converter for different values of voltage gain.

$$M_{HSU_{D < 0.5}} = \frac{1 + N}{[(1 + N) - D(1 + 2N)] + (R_L / R_o)((1 + ND)(1 + N) / 2(1 - D))} \quad (16)$$



**Fig. 9** PV connection configurations  
(a) HSU converter, (b) Cascaded boost

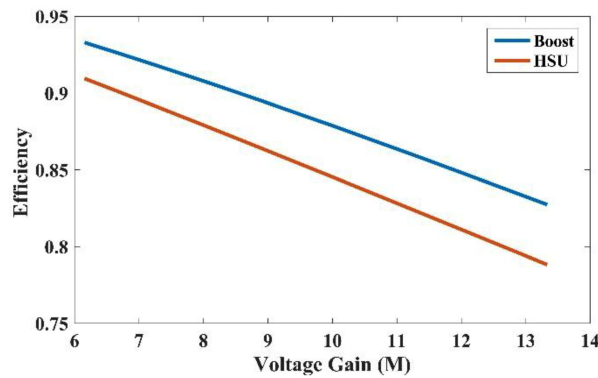


**Fig. 10** Theoretical gain vs. efficiency

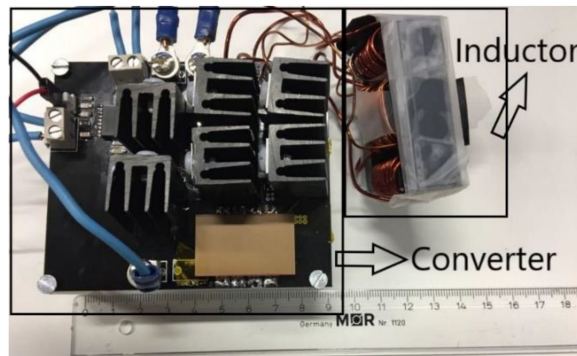


**Fig. 11** Practical prototype

#### 4 Experimental validation

Fig. 11 shows the practical prototype of the high step-up converter rated at 250 W that has been developed to obtain the test results.

To find an optimised point of operation for the high voltage gain operation, a series of tests have been performed at the HSU and cascade boost converters. Output voltage and load for all of the tests is kept constant at 200 V and 160  $\Omega$ , respectively.

Detailed parameters of the tests are given in Table 2.

As mentioned in Table 2, both HSU and cascaded boost converters are tested at different switching frequencies and the results are presented in Figs. 12 and 13, respectively.

By using a cascade boost converter, a higher gain can be achieved as compared to that with the HSU converter. The HSU converter is most efficient at low gain and 50 kHz switching frequency. Fig. 14 presents the voltage stress across the GaN

HEMT in the HSU converter for different gain values at different switching frequencies.

As the cascaded boost converter has two interleaved boost converters in series, voltage stress across the switches of the first and second converter is presented in Figs. 15 and 16, respectively.

#### 5 Conclusion

The cascaded boost converter is more efficient and can provide higher gain values than those by the HSU converter. However, at lower gain values, the HSU converter is efficient as the cascaded boost converter. However, the HSU converter has a higher energy density. So, the HSU converter is suitable for applications that have space restrictions. In the HSU converter, the average value of voltage stress across the GaN HEMT is almost equal to the input voltage, while in the cascaded boost converter, the voltage stress

**Table 2** Practical circuit parameters

output power	$P_o$	250 W
output voltage	$V_o$	200 V
switching frequency	$f_s$	50 kHz 100 kHz 150 kHz 200 kHz
duty ratio	$D$	0.3–0.7
inductance external legs	$L_1 = L_2$	302 $\mu$ H
inductance middle leg	$L_C$	2.22 mH
turns ratio	$N_C/N_1$	2
winding resistance	$R_L$	1.10 $\Omega$
load resistance	$R_o$	160 $\Omega$

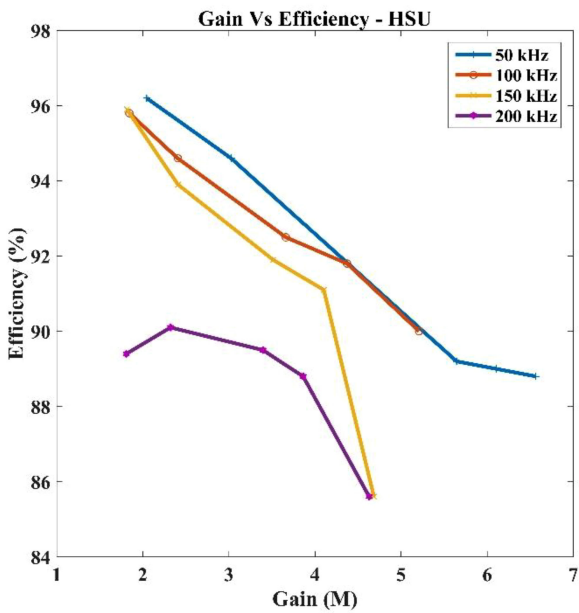


**Fig. 12** HSU experimental results

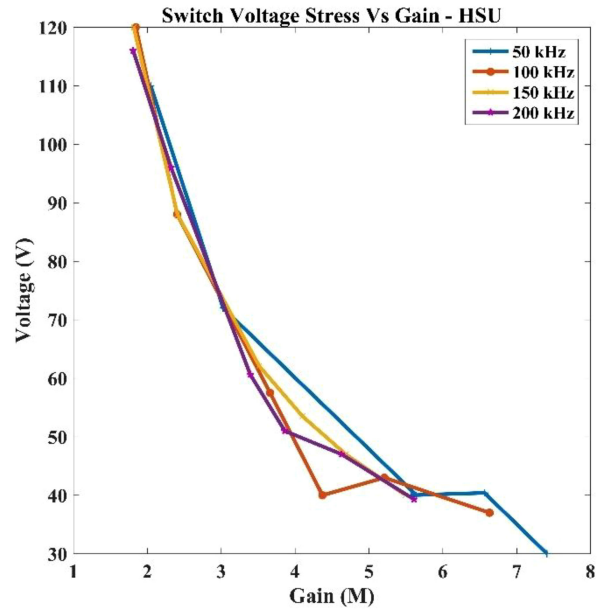


**Fig. 14** Switch voltage stress

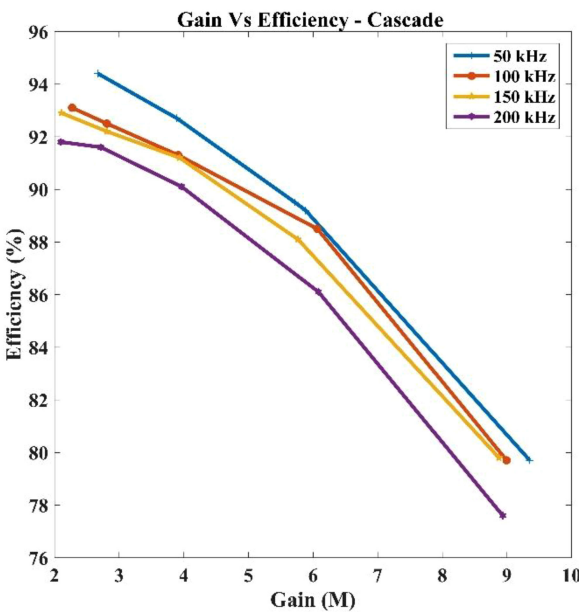


**Fig. 13** Cascade boost experimental results

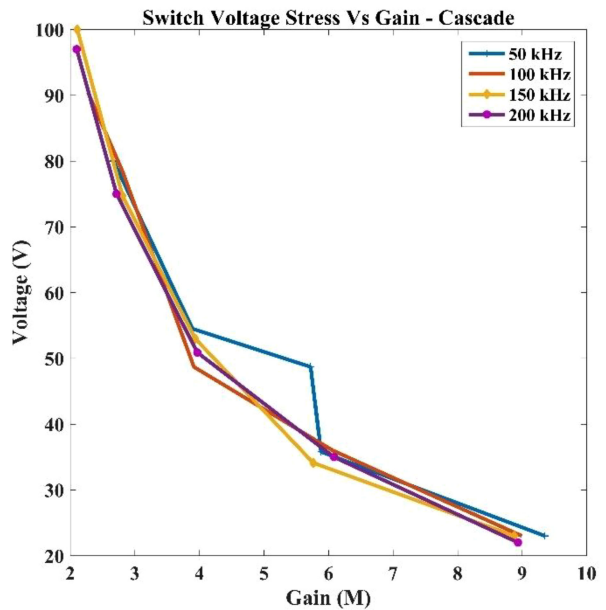


**Fig. 15** Switch voltage stress ( $S_1$ )

across the switches of the second converter is gain of the first converter times the input voltage. Hence, for the cascaded boost converter, different ratings of switches would be required for both stages.

This paper with the aid of analytical and practical analysis provided the guide to engineers to choose a step-up converter for the application.

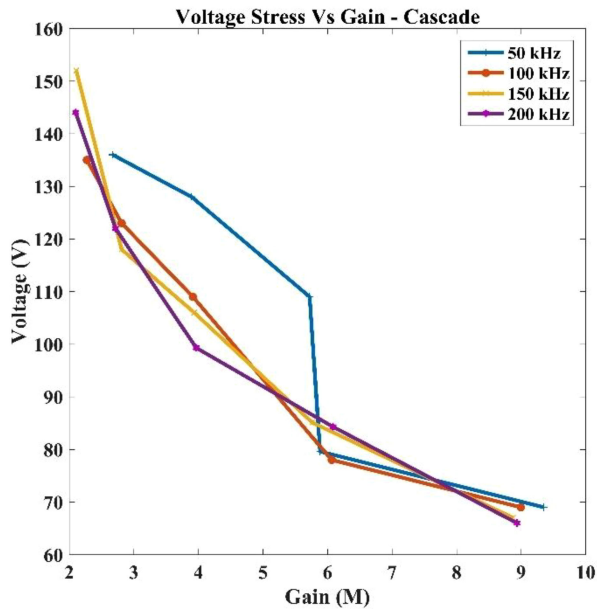


Fig. 16 Switch voltage stress ( $S_2$ )

## 6 References

- [1] Benner, J. P., Kazmerski, L.: 'Photovoltaics gaining greater visibility', *IEEE Spectr.*, 1999, **36**, (9), pp. 34–42
- [2] Myrzik, J. M., Calais, M.: 'String and module integrated inverters for single-phase grid connected photovoltaic systems—a review'. Proc. IEEE Bologna Power Tech Conf., Bologna, Italy, 2003, vol. **2**, p. 8
- [3] Pal, D., Koniki, H., Bajpai, P.: 'Central and micro inverters for solar photovoltaic integration in AC grid'. Proc. National Power Systems Conf., Bhubaneswar, India, 2016, pp. 1–6
- [4] Kjaer, S. B., Pedersen, J. K., Blaabjerg, F.: 'Power inverter topologies for photovoltaic modules – a review'. Proc. Conf. Record Industry Applications Conf., 37th IAS Annual Meeting, Pittsburgh, USA, 2002, pp. 782–788
- [5] Kjaer, S. B., Pedersen, J. K., Blaabjerg, F.: 'A review of single-phase grid-connected inverters for photovoltaic modules', *IEEE Trans. Ind. Appl.*, 2005, **41**, (5), pp. 1292–1306
- [6] Xiao, B., Hang, L., Mei, J., *et al.*: 'Modular cascaded H-bridge multilevel PV inverter with distributed MPPT for grid-connected applications', *IEEE Trans. Ind. Appl.*, 2015, **51**, (2), pp. 1722–1731
- [7] Schmitz, L., Knabben, G.C., Martins, D.C., *et al.*: 'Design optimization of a high step-up DC–DC converter for photovoltaic microinverters'. Proc. IEEE Int. Telecommunications Energy Conf., Broadbeach, Australia, 2017, pp. 432–437
- [8] Lakshmi, T. S., Rao, P. R.: 'High voltage gain boost converter for micro grid application'. Proc. Annual IEEE India Conf., Kochi, India, 2012, pp. 323–328
- [9] Cao, G., Guo, Z., Wang, Y., *et al.*: 'A high step-up modular DC/DC converter for photovoltaic generation integrated into DC grids'. Proc. Annual IEEE India Conf. – 43rd Annual Conf. IEEE Industrial Electronics Society, Beijing, China, 2017, pp. 4421–4426
- [10] Wu, G., Ruan, X., Ye, Z.: 'High step-up DC-DC converter based on switched capacitor and coupled inductor', *IEEE Trans. Ind. Electron.*, 2017, **PP**, (99), pp. 1–1
- [11] Lee, P.-W., Lee, Y.-S., Cheng, D.K.W., *et al.*: 'Steady-state analysis of an interleaved boost converter with coupled inductors', *IEEE Trans. Ind. Electron.*, 2000, **47**, (4), pp. 787–795
- [12] Liu, H. C., Li, F.: 'Novel high step-up DC–DC converter with an active coupled-inductor network for a sustainable energy system', *IEEE Trans. Power Electron.*, 2015, **30**, (12), pp. 6476–6482
- [13] Papanikolaou, N. P., Tatakis, E. C.: 'Active voltage clamp in flyback converters operating in CCM mode under wide load variation', *IEEE Trans. Ind. Electron.*, 2004, **51**, (3), pp. 632–640
- [14] Martinez, W., Imaoka, J., Yamamoto, M., *et al.*: 'High step-up interleaved converter for renewable energy and automotive applications'. Proc. Int. Conf. Renewable Energy Research and Applications, Palermo, Italy, 2015, pp. 809–814
- [15] Martinez, W., Imaoka, J., Itoh, Y., *et al.*: 'Analysis of coupled-inductor configuration for an interleaved high step-up converter'. Proc. 9th Int. Conf. on Power Electronics and ECCE Asia (ICPE-ECCE Asia), Seoul, South Korea, 2015, pp. 2241–2248
- [16] Martinez, W., Cortes, C.A., Imaoka, J., *et al.*: 'Current ripple modeling of an interleaved high step-up converter with coupled inductor'. Proc. IEEE 3rd Int. Future Energy Electronics Conf. and ECCE Asia, Kaohsiung, Taiwan, 2017, pp. 1084–1089
- [17] Martinez, W., Cortes, C.A., Yamamoto, M., *et al.*: 'Effect of inductor parasitic resistances on the voltage-gain of high step-up DC-DC converters for electric vehicle applications', *IET Power Electron.*, 2018, **11**, (10), pp. 1628–1639